J Biosci (2024)49:56
DOI: 10.1007/s12038-023-00416-5

Review

Systems biology of plant metabolic interactions

Devlina Sarkar and Sudip Kundu*

Department of Biophysics, Molecular Biology and Bioinformatics, University of Calcutta, Kolkata, India

**Corresponding author (Email, skbmbg@caluniv.ac.in)*

MS received 31 May 2023; accepted 3 October 2023

Metabolism is the key cellular process of plant physiology. Understanding metabolism and its dynamical behavior under different conditions may help plant biotechnologists to design new cultivars with desired goals. Computational systems biochemistry and incorporation of different omics data unravelled active metabolism and its variations in plants. In this review, we mainly focus on the basics of flux balance analysis (FBA), elementary flux mode analysis (EFMA), and some advanced computational tools. We describe some important results that were obtained using these tools. Limitations and challenges are also discussed.

Keywords. Elementary flux mode analysis; flux balance analysis; metabolic interactions; mitochondria; regulations; systems biochemistry

1. Introduction

Metabolism is the key process of any living organism that comprises a series of chemical reactions involved in building up sugars and other molecules by photosynthesis utilizing smaller molecules and producing energy by respiration from those complex biological molecules, such as proteins, lipids, nucleic acids, carbohydrates, etc., to sustain life. In the case of plant systems, the term 'metabolism' directly points towards some cellular processes such as glycolysis, the tricarboxylic acid cycle (TCA cycle), the Calvin cycle, the pentose phosphate pathway, the electron transport chain, etc., which take place in the cytosol and other different cellular compartments such as mitochondria, chloroplasts, and peroxisomes. Most of the reactions of metabolic pathways are catalyzed by different enzymes, and therefore, they can be regulated by varying the activities of those enzymes. On the other hand, there are other factors like substrate and product concentrations, as well as ion concentrations, that act as co-factors for different enzymes, pH levels, genomic and transcriptomic variations, and stress conditions which can up- or down-regulate metabolic pathways. Several important pathways of central carbon metabolism occur within plant mitochondria and synthesis the important players. Various shuttle systems and transporters help mitochondria maintain their interactions with the cytosol, chloroplast, peroxisome, etc. In this review, we focus on mitochondrial metabolism and its interactions with other cellular compartments and their regulations. In the following sections, we will elaborate on the computational approaches that can integrate different omics and simulation data to understand metabolic interactions at the cellular level. Flux balance analysis (FBA) (Orth *et al.* 2010) is one of the important mathematical constraint-based modeling approaches to understand flux distributions in metabolic networks under different cellular conditions. Regulation of metabolism due to differential gene expressions and variations in enzyme concentrations can be analyzed by modifying the classical FBA method. Flux variability analysis (FVA) may indicate new feasible pathways which can be then validated

This article is part of the Topical Collection: Plant Mitochondria: Properties and Interactions with Other Organelles.

http://www.ias.ac.in/jbiosci
Published online: 07 May 2024

either through proteomics or gene expression data, i.e., whether under different conditions these different sets of metabolic pathways get activated. Furthermore, elementary flux mode analysis (EFMA) (Schuster *et al*. 1999) gives us alternative modes of different metabolic pathways. The flux coupling finder (FCF) (Burgard *et al*. 2004) can indicate coupled metabolic reactions, i.e., whether a change in one reaction will result in a corresponding change in a coupled reaction.

2. Biochemical pathways of biomass production in plant leaves

Incident light energy is converted to chemical energy in the form of adenosine triphosphate (ATP) and nicotinamide adenine dinucleotide phosphate hydrogen (NADPH) by the two photosystems – I and II, embedded in the thylakoid membrane of chloroplasts. These reactions, occurring in the presence of light, are called light reactions (Arnon 1971). The ATP and NADPH produced by light reactions enter the Calvin–Benson cycle, which takes place in the stroma of the chloroplast. The main enzyme that works in the Calvin–Benson cycle is ribulose-1,5-bisphosphate carboxylase/oxygenase (RuBisCO) (Sharkey 2023). Three molecules of ribulose-1,5-bisphosphate (RuBP) and three molecules of CO_2 enter the cycle and generate six molecules of glyceraldehyde-3-phosphate (GAP). One molecule is released and gets utilized in the production of glucose, and the remaining are used in regenerating three molecules of RuBP. The sugar produced in the chloroplast enters the glycolytic pathway in the cytosol, where both GAP and glucose are converted to pyruvate as the end product of this pathway. Now, pyruvate leaves the cytosol, and the mitochondrion comes into play. In the next section, we discuss mitochondrial metabolism in detail. Mitochondrial metabolism and its interactions with other organelles are described schematically in figure 1.

2.1 *Mitochondrial metabolism*

Mitochondrial metabolism is closely related to cytosolic and chloroplastic metabolisms, and a major part of mitochondrial metabolism is covered by the TCA cycle (also known as the citric acid or Krebs cycle), the electron transport chain (ETC), and ATP synthesis. These metabolic pathways can also be regulated in different ways. A schematic overview of the regulations of mitochondrial metabolism is shown in figure 2.

Either pyruvate, the end product of glycolysis, enters the mitochondrial matrix directly with the help of mitochondrial pyruvate carriers (MPC) present in the inner mitochondrial membrane, or the mitochondrial NAD-malic enzyme (NAD-ME) synthesizes pyruvate inside mitochondria by oxidatively decarboxylated malate, which is derived from phosphoenolpyruvate (PEP) (Rustin *et al*. 1980). It can also be synthesized from alanine with the help of alanine aminotransferase inside the mitochondrial matrix (Le *et al*. 2022). Oxaloacetate (OAA) is produced by cytosolic PEP carboxylase, followed by the production of malate, and both metabolites are transported to the mitochondrion to maintain the pyruvate pool inside the mitochondrial matrix (Zoglowek *et al*. 1988; Hanning *et al*. 1999). In the mitochondrial matrix, pyruvate is converted to acetyl CoA by oxidative decarboxylation through the action of the mitochondrial pyruvate dehydrogenase complex (PDC), which releases CO_2 and reduces NAD^+ to NADH (Tovar-Méndez *et al*. 2003; Araujo *et al*. 2012). Acetyl CoA is also used in the fatty acid biosynthesis. Acetyl CoA can be derived, depending on the organism and cell type, from β-oxidation of fatty acids or from the degradation of ketogenic amino acids (Sweetlove *et al*. 2010). Mitochondrial PDC is inhibited by acetyl CoA (Tovar-Méndez *et al*. 2003) and light (Poolman *et al*. 2013), and activated by thiamine pyrophosphate (Bocobza *et al*. 2013).

2.1.1 TCA cycle: The TCA cycle comprises a series of eight oxidative steps that release two carbon atoms as CO_2 and generate NADH and $FADH_2$, which are further used in the mitochondrial ETC. The condensation of oxaloacetate (OAA) and acetyl CoA by citrate synthase (CS) occurs in the first step of the TCA cycle to produce citrate. The enzyme citrate synthase is regulated by oxidation and reduction of cysteine residues present in the enzyme (Nishio and Mizushima 2020). Thioredoxins (TRX) reduce the intra- and intermolecular disulfide bonds of the enzyme and form the active dimer of the enzyme (Schmidtmann *et al*. 2014). An increase in enzyme activity is also observed when it gets reduced with dithiothreitol (DTT) (Stevens *et al*. 1997). In response to light, its activity increases by 1.4-fold (Unger and Vasconcelos 1989) and hydrogen peroxide (Schmidtmann *et al*. 2014), and diamide (Stevens *et al*. 1997) can decrease the activity of the enzyme by 54% and 25%, respectively, due to the formation of mixed disulfides by oxidation. This enzyme is again inhibited by higher temperature (50°C)

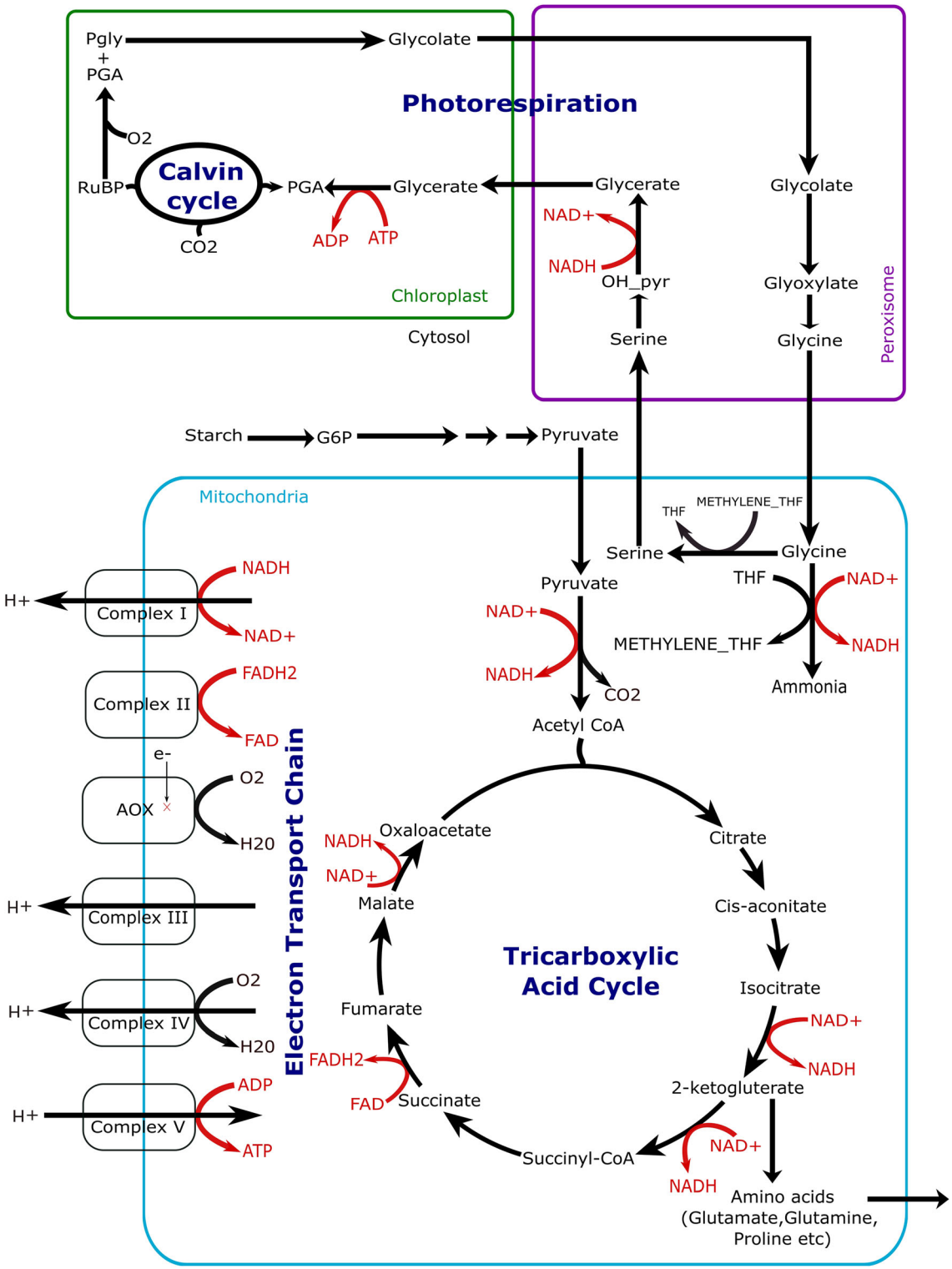

Figure 1. Schematic representation of plant metabolism including four compartments: cytosol, mitochondrion, peroxisome, and chloroplast. This includes a brief overview of the following metabolic pathways: (i) mitochondrial tricarboxylic acid cycle (TCA cycle) producing reductants and amino acid precursors, (ii) mitochondrial electron transport chain (ETC) producing ATP, (iii) chloroplastic Calvin–Benson cycle (C_3 cycle) that generates one molecule of the three carbon sugar, glyceraldehyde-3-phosphate, and (iv) photorespiration (C_2 cycle) which spans all the four compartments and is involved in protecting the cell from photoinhibition.

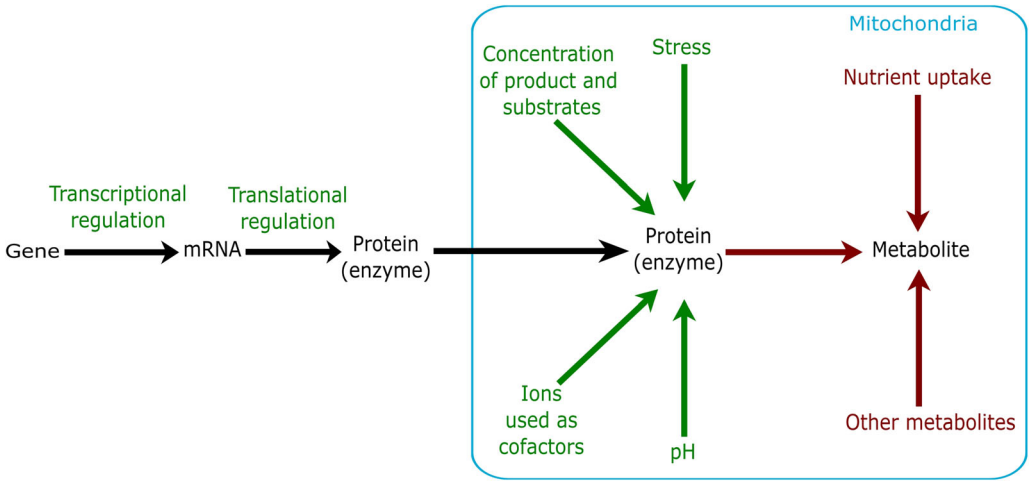

Figure 2. Different regulations of mitochondrial metabolism.

and higher concentration of ATP, NADH, succinyl-CoA, citrate, and 2-oxoglutarate (Alejandre *et al*. 1979) and activated by ADP (Barbareschi *et al*. 1974; Siedow and Day 2000).

Citrate is converted to isocitrate by aconitase via the bound intermediate *cis*-aconitate. The important metabolites of the TCA cycle, fumarate, malate, succinate, and *trans*-aconitate, have little inhibitory control over the enzyme aconitase. In the presence of light, succinate dehydrogenase gets inhibited, which results in the accumulation of succinate. The increased level of succinate causes inhibition of mitochondrial aconitase, which stimulates the efflux of citrate from mitochondria (Eprintsev *et al*. 2015). Previous studies have also shown that a few more events, such as the presence of nitric oxide (Gupta *et al*. 2012) and a plant metabolite, citramalate (Sipari *et al*. 2020), lack of manganese superoxide dismutase (Morgan *et al*. 2008), and accumulation of H_2O_2 in mitochondria due to the suppression of the mitochondrial ETC, can inhibit the activity of aconitase (Verniquet *et al*. 1991; Nunes-Nesi *et al*. 2013). Its activity gets completely blocked at 50 μM H_2O_2 (Tretter and Adam-Vizi 2000).

In the next step, NAD- or NADP-dependent isocitrate dehydrogenases (NAD-ICDH/NADP-ICDH) oxidatively decarboxylate isocitrate to 2-oxoglutarate and generate CO_2 and NADH or NADPH, respectively. NAD-ICDH found only in mitochondria (Lancien *et al*. 1998) is inhibited by NADH (in a competitive manner) (McIntosh and Oliver 1992) and high concentration of isocitrate (Popova and de Carvalho 1998). On the other hand, NADP-ICDH found in mitochondria, plastids, peroxisomes, and cytosol (Hodges *et al*. 2003) is inhibited by NADPH non-competitively (McIntosh and Oliver 1992; Igamberdiev and Gardeström 2003). Citrate regulates the enzyme in a competitive manner: at low isocitrate concentrations, activation occurs by citrate, but at high isocitrate concentrations, citrate appears to be a competitive inhibitor (Cox and Davies 1969). Various organic acids (2-oxoglutarate, citrate, *cis*- and *trans*-aconitate, gly-oxylate, and oxaloacetate), ions of metals (Mn^{2+}, Mg^{2+}, Zn^{2+}, etc.), and some nucleoside phosphates such as ATP regulate the activities of NAD-ICDH and NADP-ICDH (McIntosh and Oliver 1992; Popova and de Carvalho 1998). A previous study showed that the activity of NAD-ICDH present in pumpkin cotyledon is increased by 15% at pH 7.2 and by 70% at pH 8.0 at optimal citrate concentration of 0.5 mM (Popova and de Carvalho 1998).

Another oxidative decarboxylation reaction occurs when succinyl CoA is generated from 2-oxoglutarate, generating CO_2 and NADH as by-products. The reaction is catalyzed by the enzyme 2-oxoglutarate dehydrogenase complex (OGDHC), which is regulated by the levels of both its substrates, i.e., 2-oxoglutarate and NADH and products, i.e., succinyl-CoA, and some other factors, such as Ca^{2+}, ATP/ADP, NADH/NAD^+, and thiamine pyrophosphate (Wedding and Black 1971; Strumilo 2005; Bunik and Fernie 2009).

Succinyl-CoA ligase (ScoAL), also called succinate thiokinase or succinyl-CoA synthetase, subsequently catalyzes the synthesis of succinate from succinyl-CoA along with the formation of ATP from ADP and P_i. Low concentration of 2-oxoglutarate activates the enzyme, whereas citrate, isocitrate, succinate, fumarate, malonate, and intermediates of the porphyrin biosynthesis pathway (Palmer and Wedding 1966) inhibit the enzyme at their high concentrations (Studart-Guimarães *et al*. 2005).

Next, succinate dehydrogenase (SDH) combines two reactions: the oxidation of succinate to fumarate and the reduction of ubiquinone to ubiquinol. The latter is an essential step for transferring electrons from redox equivalents to oxygen during the process of the ETC. SDH is also known as complex II, a major component of the ETC. Both ATP and ADP can activate the enzyme. On the other hand, the activity of the enzyme is negatively affected by potassium (Affourtit *et al*. 2001), TRX (Daloso *et al*. 2015), and nitric oxide (NO) (Simonin and Galina 2013).

In the next step, fumarate is reversibly converted to malate by hydration/dehydration. The investigation of regulation of fumarase from pea (*Pisum sativum* L.), reveals that the alpha-keto acids pyruvate and 2-oxoglutarate at millimolar concentrations and the adenine nucleotides ATP, ADP, and AMP can inhibit the enzyme (Behal and Oliver 1997). However, the enzyme gets activated by Mg^{2+}, K^{+}, and Ca^{2+} (Eprintsev *et al*. 2018) and deactivated by TRX (Daloso *et al*. 2015).

In the last step of the cycle, malate is oxidized to oxaloacetate by a reversible reaction catalyzed by NAD-dependent malate dehydrogenase. It is likely that accumulation of NADH leads to an inhibition of the mitochondrial malate dehydrogenase (Nunes-Nesi *et al*. 2013). At low malate concentration, this enzyme appears to be most active (Wedding *et al*. 1976).

The two most important shuttles – malate-aspartate and malate-OAA – use malate (Zoglowek *et al*. 1988) for the transport of substrate and redox equivalents across the mitochondrial membrane to maintain the redox balance in the cell. The cycle not only generates the reducing equivalents NADH and $FADH_2$ to synthesize ATP by oxidative phosphorylation through the ETC, but also supplies carbon skeletons for the synthesis of different biological compounds. For example, 2-oxoglutarate acts as a precursor for amino acid biosynthesis.

2.1.2 Electron transport chain and ATP synthesis: Oxidative phosphorylation comprises two important processes, the ETC and ATP synthesis. It generates ATP by using the redox equivalents NADH and $FADH_2$ from the TCA cycle.

The electron transport chain is made up of four enzyme complexes present within the inner membrane of mitochondria. The high energy electrons are transferred from the reducing equivalents NADH and $FADH_2$ through a series of reactions to oxygen, the final electron acceptor, by losing its energy, which is used to pump out protons from the matrix into the inter-membrane space. Complex I, also known as NADH dehydrogenase, and complex II, also known as succinate dehydrogenase, accept two electrons from NADH and $FADH_2$, respectively. They cause the oxidation of NADH and $FADH_2$, respectively, and pass the electrons to complex III (Q-cytochrome c oxidoreductase), the first cytochrome (cyt) in the pathway, via coenzyme Q (also known as quinone and CoQ). Complex IV passes the electrons to oxygen, which generates water. Complex I, III, and IV release $4H^{+}$, $4H^{+}$, and $2H^{+}$ into the intermembrane space, respectively, while complex II does not directly pump any protons out. Hence, a concentration difference of protons (higher in the intermembrane space than the matrix), i.e., a pH gradient, is developed across the membrane. A voltage gradient is also developed due to the difference of charge. These two collectively constitute an electrochemical gradient (equivalent to $\sim$150–200 mV) which exerts a proton motive force (pmf) across the inner mitochondrial membrane and this pmf is used by the enzyme ATP synthase, a multi-protein complex, to generate ATP.

The generation of one ATP molecule requires four protons (three protons go through ATP synthase and one is used for the transport of P_i and ADP into mitochondria). ATP synthase is made up of two components, F_O (rotor), and F_1 (catalytic head and stalk) (Seelert and Dencher 2011). F_O is a transmembrane protein complex, embedded in the inner mitochondrial membrane, which accepts protons and rotates the F_1 head. A complete rotation of ATP synthase transfers ten protons from the intermembrane space to the matrix and generates three ATP molecules. These ATP molecules are utilized for different cellular activities and survival of the cell.

2.1.3 Alternative oxidase: In addition to cytochrome oxidase, mitochondria contain an alternative oxidase (AOX) that directly couples the oxidation of ubiquinol with the reduction of O_2 to H_2O without proton translocation from the matrix to the mitochondrial inter-membrane space (Jacoby *et al*. 2012). High-energy electrons are partitioned between two paths in the ETC: the cytochrome pathway (complex III, cyt c, complex IV) and AOX. Notably, AOX bypasses the flow of electrons through complexes III and IV, prohibiting the excessive reduction of the downstream complexes of the ETC and thus dissipates the free energy of electrons in the form of heat (Moore and Siedow 1991; Rhoads and Subbaiah 2007). This reduces the level of ATP synthesis. However, if AOX takes electrons from NADH, a diminished amount of

ATP is still synthesized as these electrons arise via the proton pumping complex I. Therefore, if $FADH_2$ provides the electron flow to AOX, the electron flow will be completely uncoupled from ATP turnover since complex II, unlike complex I, is not proton-pumping. Briefly, the mitochondrial ETC can dramatically modulate the production of ATP depending on the components of the path used for electron flow to cope with different physiological conditions (Millar *et al*. 2011).

The alternative oxidase is located in the inner mitochondrial membrane in a dimeric form. The dimer exists in two different states: an oxidized state, in which the dimer is covalently cross-linked by an intermolecular disulfide bridge, and a reduced state, in which the disulfide bond is reduced to its component sulfhydryls and non-covalent interactions maintain the dimeric structure of AOX (Moore *et al*. 1995). The oxidized form is four- to five-fold less active than the reduced form, and the two forms are regulated by reversible oxidation-reduction of the cysteine bond between two monomers (Umbach and Siedow 1993). An increase in reducing equivalents (NADH, NADPH) can activate AOX (Sluse and Jarmuszkiewicz 1998). AOX can be activated by pyruvate (Pastore *et al*. 2001) and succinate (Vanlerberghe and McIntosh 1997; Sluse and Jarmuszkiewicz 1998; Saha *et al*. 2016). Electron transfer between cyt oxidase and AOX can be affected by the level of ubiquinone concentration. In the absence of ADP or in the presence of cytochrome chain inhibitors such as nitric oxide (NO), carbon monoxide (CO), hydrogen sulfide (H_2S), hydrogen cyanide (HCN), etc., the cytochrome pathway activity becomes low and AOX gets activated (Sluse and Jarmuszkiewicz 1998; Cooper and Brown 2008). AOX activity can be altered in response to stress (Vanlerberghe 2013). Temperature has an effect on AOX activity in plants (Campbell *et al*. 2007; Armstrong *et al*. 2008; Searle *et al*. 2011; Shi *et al*. 2013). In a study, it was reported that in a callus culture of *Arabidopsis*, shifting to a chilling temperature in addition to ethylene treatment was required to induce AOX activity (Wang *et al*. 2012). Furthermore, higher amount of AOX protein was seen in *Arabidopsis* grown at 12°C than warm grown plants, and knockdown plants with low AOX levels showed no growth in low temperatures (Fiorani *et al*. 2005). Similarly, when chilling-sensitive maize was given a short-term cold treatment (5 days at 5°C), the respiration shifted its usage from cyt oxidase to AOX in such a way that, in the new condition, 60% of total respiration occurred through AOX (Ribas-Carbo *et al*. 2000). Furthermore, cyt activity was found to be reduced and AOX activity was increased in tobacco in response to ozone treatment (Ederli *et al*. 2006). A shift from cyt oxidase to AOX oxidase was observed in response to high light intensity (Poolman *et al*. 2013).

2.1.4 Interactions of mitochondria with other organelles through photorespiration: Photorespiration is a wasteful but important biological process which includes a light-dependent uptake of O_2 and release of CO_2 and limits plant growth by regulating the photosynthetic electron flow in different light intensities (Huang *et al*. 2015). It is called a wasteful process because it does not generate ATP or sugar. Ribulose-1,5-bisphosphate carboxylase/oxygenase (RuBisCO), the main enzyme of the Calvin–Benson cycle, is a bifunctional enzyme since it catalyzes carboxylation and oxygenation of ribulose-1,5-bisphosphate (RuBP). One molecule of 2-phosphoglycolate is produced when O_2 interacts with RuBisCO. Phosphoglycolate accumulation in the cell is toxic as it prevents different important steps of the central carbon metabolism by inhibiting two enzymes, triose-phosphate isomerase and sedoheptulose-1,7-bisphosphate phosphatase (Flugel *et al*. 2017). Phosphoglycolate is recycled by converting to phosphoglycerate through photorespiration, which is also known as the C_2 cycle or glycolate cycle or oxidative photosynthetic carbon cycle (Leegood *et al*. 1995). It involves a series of enzymatic reactions in the peroxisome, mitochondrion, and chloroplast (Oikawa *et al*. 2019). 2-Phosphoglycolate is dephosphorylated by glycolate-2-phosphatase within the chloroplast to form glycolate and this reaction recycles P_i within the chloroplast. Glycolate then leaves the chloroplast and gets oxidized by glycolate oxidase inside the peroxisome and generates glyoxylate along with the generation of hydrogen peroxide, which is then decomposed in the peroxisome by catalases. Serine-glyoxylate aminotransferase (SGAT) and glutamate-glyoxylate aminotransferase (GGAT) then convert glyoxylate to glycine. Glycine then moves to the mitochondrion from the peroxisome and is oxidized to ammonia and serine by glycine decarboxylase (GDC) with the help of another enzyme called serine hydroxymethyltransferase 1 (SHMT1) (Neuburger *et al*. 1986). Regulation of GDC is important, as a previous study showed that the increased activity of the GDC enhances net photosynthesis and growth of *Arabidopsis thaliana* (Timm *et al*. 2012). Mitochondrial NADH/NAD^+ ratios regulate GDC activity *in vivo* (Bourguignon *et al*. 1988; Igamberdiev and Gardeström 2003) and mitochondrial thioredoxins (Trx) Trx o1 (Reinholdt *et al*. 2019) and Trx h2 (da

Fonseca-Pereira *et al*. 2020) regulate photorespiratory carbon flow from chloroplasts to mitochondria by regulating GDC activity (Timm and Hagemann 2020). In the next step, serine is then transported to the peroxisome and is converted to glycerate, and in this form the chloroplast gets its photorespiratory carbon. Glycerate kinase phosphorylates glycerate and generates phosphoglycerate that re-enters the photosynthesis cycle (Ogren 1984).

3. Different simulation techniques to analyze regulations of metabolism

The active metabolism within different cellular compartments and their variations can be analyzed using different approaches of metabolic flux analysis (such as flux balance analysis and elementary flux mode analysis) and flux coupling analysis. The metabolic modeling techniques can be grouped into two categories: (i) kinetic modeling (Rohwer 2012) and (ii) structural modeling (Schuster and Fell 2007). The details of the different kinetic properties of different enzymes involved in a network are required for kinetic modeling. Therefore, these huge requirements limit its application to small systems having small number of reactions. However, only limited experimental data are required for structural modeling, such as the stoichiometry and reversibility of all biochemical reactions that participate in the network, the uptake rates of essential nutrients, and the biomass composition of the cell, tissue, or organism (Lotz *et al*. 2014). Thus, the structural modeling technique is widely used in genome-scale metabolic modeling and its analysis. Genome-scale metabolic models (GSMs) of different organisms, including bacteria, simple eukaryotes, and plants, are now available.

Researchers have reconstructed several genome-scale metabolic models to analyze both C_3 and C_4 plant metabolisms. This list includes *Arabidopsis* (*Arabidopsis thaliana*) (Poolman *et al*. 2009; de Oliveira Dal'Molin *et al.* 2010; Mintz-Oron *et al*. 2012), rice (*Oryza sativa*) (Poolman *et al*. 2013), maize (*Zea mays*) (Saha *et al*. 2011), tomato (*Solanum lycopersicum L.*) (Yuan *et al*. 2016), soybean (*Glycine max*) (Moreira *et al*. 2019), and *Setaria viridis* (Shaw and Cheung 2019). Moreover, there was an earlier effort to reconstruct a genome-scale metabolic model (C4GEM) (de Oliveira Dal'Molin *et al.* 2010) to study general C_4 plant metabolism using the reactions of maize (*Zea mays*), sorghum (*Shorghum bicolor*), and sugarcane (*Saccharum officinarum*).

3.1 *Flux balance analysis*

Flux balance analysis (FBA) is a constraint-based modeling approach that allows the identification of optimal flux through the reactions of a metabolic network in a steady state by applying mass balance constraint to the stoichiometric model and maximizing or minimizing the objective function, defined according to the desired objective (Orth *et al*. 2010; Lotz *et al*. 2014). The metabolic reactions and the objective are mathematically represented by a system of linear equations, and these equations are solved using linear programming. As this approach does not require the kinetic parameters of the enzymes involved in the system, even for large networks, FBA can be computed very quickly. This method is used to predict all possible flux distributions of a specific system for different environmental and physiological conditions of the system (Orth *et al*. 2010).

In the first step, reactions of a metabolic network are represented in the form of a stoichiometry matrix, **S** of size $m \times n$, where m represents the number of metabolites and n represents the number of reactions of the network. The elements of each column represent the stoichiometric coefficients of the substrates and products of the corresponding reaction. A negative value is given to a substrate that is being consumed, a positive value is given to a product that is being produced, and zero represents a metabolite that is absent in that particular reaction.

At steady state, the rate of production and the rate of consumption are equal for each internal metabolite in the model and that can be mathematically represented as

$$\mathbf{Sv} = 0$$

where the vector **v** represents the flux through all the n number of reactions and **S** is the stoichiometry matrix. The optimization problem can be defined as

$$\text{maximize or minimize } \mathbf{z} = \mathbf{c}^T\mathbf{v}$$

The flux constraints are given as

$$\mathbf{c}_l \leq \mathbf{v} \leq \mathbf{c}_u$$

where **z** is the objective function, $\mathbf{c}^T$ is the transpose of a vector (**c**) of weights that indicate how much a reaction contributes to the objective, **v** is the vector of all fluxes, **S** is the stoichiometry matrix, and $\mathbf{c}_l$ and $\mathbf{c}_u$ are the vectors of lower and upper bound of fluxes, respectively. In the case of an irreversible reaction, the lower bound $\mathbf{c}_l$ becomes 0 and the allowable flux is

limited to be greater than or equal to 0. The method is schematically described in figure 3.

3.2 *Elementary flux mode analysis*

Another structural modelling technique is the elementary flux mode analysis (EFMA) (Schuster *et al.* 1999). It is a mathematical tool in which the metabolic network is decomposed into several elementary modes, which cannot be further broken. By definition, an elementary mode is a set of reactions that cannot be decomposed further. Any feasible route of a metabolic network from a substrate to a product can be represented as a linear combination of elementary modes.

All reactions of the metabolic network and the information whether they are reversible or irreversible can be represented mathematically as a matrix, called a stoichiometry matrix, **S**, in which the rows represent the reactions and the column represent the internal metabolites. The reactions which always operate together are lumped to reduce the size of the matrix.

The first step to compute elementary modes of the metabolic network is the construction of initial tableau, $\mathbf{T}^0$, which is a matrix formed by creating a transposed matrix of the stoichiometry matrix **S**, and augmented by the identity matrix, **I**.

$$\mathbf{T}^0 = \left(\mathbf{S}^T|\mathbf{I}\right)$$

In the next step, from $\mathbf{T}^0$ we compute a second tableau $\mathbf{T}^1$ in which we obtain a null vector for the first column, i.e., all the elements of the first column are 0, by pairwise linear combination of rows. By this process, for all the columns of the transposed stoichiometry matrix, null vectors are obtained consecutively.

In the final tableau there is a null matrix on the left-hand side, and the identity matrix on the right-hand side is now replaced by a matrix of elementary modes. Each row of the matrix represents a specific elementary mode. A linear combination of two or more elementary modes corresponds to a steady state flux distribution of the network.

3.3 *Flux coupling analysis*

Flux coupling finder (FCF) is a procedure to find the blocked and coupled reactions in the genome-scale metabolic system. Like EFMA, it does not require computation of null-space matrices, which is a problematic task for large networks. Instead, it requires the

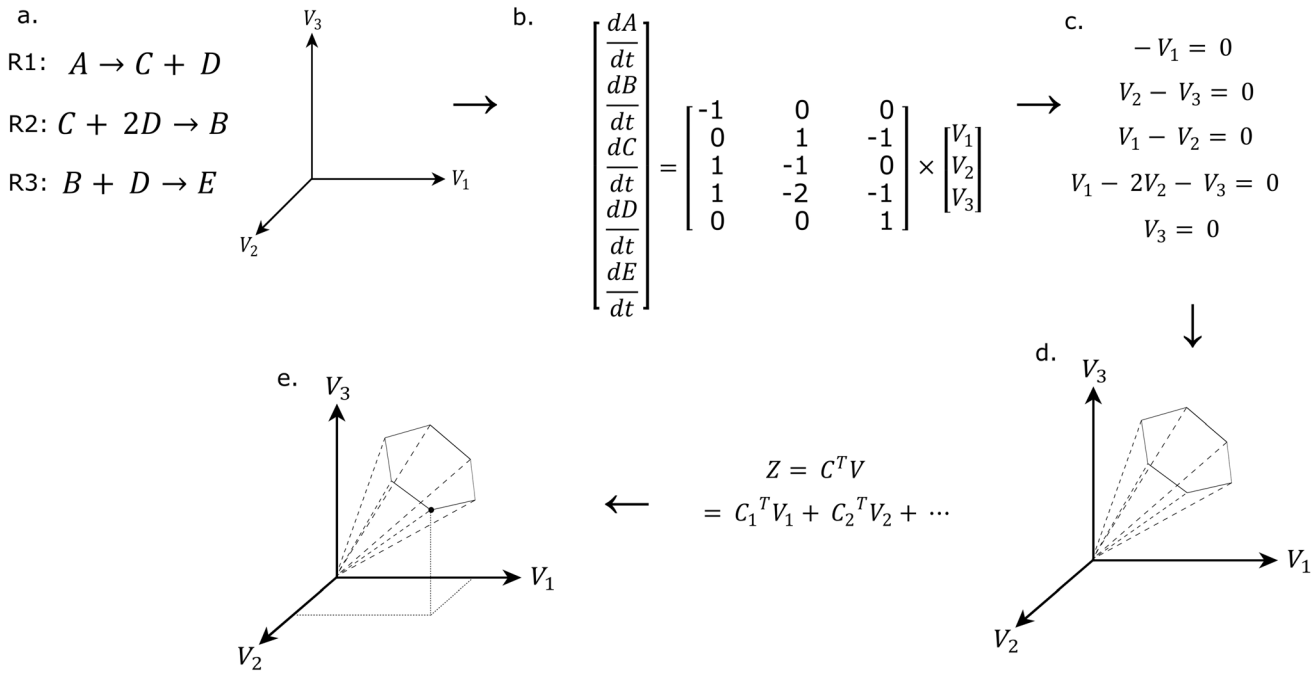

Figure 3. Schematic overview of the method of flux balance analysis: (**a**) We have considered three reactions (R1, R2, and R3) of a metabolic network, and at the beginning the solution space is unconstrained; (**b**) reactions are then represented in a form of stoichiometry matrix, S; (**c**) reactions at steady state are represented in the form of fluxes; (**d**) allowable solution space after applying constraints; and (**e**) optimal solution after optimizing the objective function, i.e., minimizing or maximizing it using linear programming.

solution of a sequence of linear programs (LPs) (Burgard *et al*. 2004).

By solving the linear programming problem, we can easily identify the blocked reactions by identifying the reactions having 0 as maximum flux value. Blocked reactions are those which are incapable of carrying any flux under steady state condition. Here, limitation of the uptake of resources, i.e., carbon, nitrogen, etc., and transport of the metabolites out of the cells are used as constraints (Burgard *et al*. 2004).

Coupled reactions can be identified by calculating the maximum and minimum flux ratios (F_{max} and F_{min}), where $F=x_1/x_2$ for every pair of metabolites (x_1 and x_2) and F_{min} and F_{max} represent minimum x_1/x_2 and maximum x_1/x_2, respectively. Results can infer the following:

1. When F_{min}=0, F_{max}=C, a finite value, the fluxes are directionally coupled, i.e., a non-zero flux of one reaction (x_1) implies a non-zero for another reaction (x_2) but not the reverse,
2. When F_{min}=c, a finite value, F_{max}=infinite, the fluxes are directionally coupled but in the opposite direction in comparison with the previous result i.e., the non-zero flux of the second reaction (x_2) implies a non-zero flux for the 1st reaction (x_1).
3. If F_{min} and F_{max} both are finite but unequal, the fluxes are partially coupled, that is, a non-zero flux for one reaction (x_1) implies a non-zero but variable flux through another reaction (x_2) and vice versa
4. If F_{min} and F_{max} both are finite and equal, the fluxes are fully coupled, i.e., a non-zero flux for one reaction (x_1) implies a non-zero and a fixed flux through another reaction (x_2) and vice-versa
5. If F_{min} and F_{max} vary from 0 to infinity, the fluxes are uncoupled.

The equivalent knockouts, i.e., the reactions whose deletion causes the flux of a particular reaction to be 0 and the affected reactions, i.e., the reactions whose fluxes become 0 after deleting a particular reaction, can also be identified by this approach.

4. Application of the previously described approaches for analyzing metabolic interactions

4.1 *Application of flux balance analysis (FBA) to analyze the metabolic interactions in plants*

4.1.1 Can we identify active metabolic pathways working in different cellular conditions using FBA? Metabolism can be defined as the combination of a number of metabolic pathways that occur within a cellular system. All the reactions of different pathways of a cell may or may not be acting together at a time. FBA gives us the optimal flux distributions through the reactions in different cellular conditions by solving biochemical networks using linear programming. Different objective functions are used according to the phenotype of interest. For example, biomass production is used as an objective function in predicting growth. Moreover, different cellular conditions can be applied to a model by applying constraints such as changing the bounds of the flux values of the reactions (Orth *et al*. 2010). In a previous study (Chatterjee *et al*. 2017) on the genome-scale model of *Oryza sativa indica*, the effect of gradually increasing photorespiration, which can be represented as high to low ratios of carboxylase and oxygenase activity of RuBisCO, was analyzed by fixing its ratio during model simulations. Here, the objective function used was minimization of total cellular flux while producing biomass components in an experimentally fixed proportion. The result showed that the photon demand for the production of ATP and NADPH to synthesize biomass decreases with a decrease in photorespiration. They also reported that cyclic photophosphorylation is active only when photorespiration is high, whereas non-cyclic photophosphorylation is always active (Chatterjee *et al*. 2017).

4.1.2 Is it possible to capture the feasible alternative pathways and variations in reactions occurring in different cellular compartments when a reaction is not working completely or partially inside the cell? The knockout or complete inhibition of a reaction resembles deletion of that reaction from a metabolic model and can be done by fixing its flux value to zero. This *in silico* reaction deletion strategy has been used along with FBA on a genome-scale metabolic model of rice leaf to identify the essential reactions of the model (Shaw and Kundu 2015). Reactions that are so important for a model that deletions of them inhibit the synthesis of biomass are called essential reactions. For example, the light-dependent non-cyclic reaction has been reported as an essential reaction as it should be active in every condition of cell in order to produce ATP and NADPH, required for the synthesis of biomass. Another essential reaction is the carboxylase reaction of RuBisCO, without which the cell cannot fix CO_2 for the production of biomass. The O_2 and CO_2 transporters are also essential, as they are necessary for plant survival and biomass production.

This study of metabolic plasticity has also successfully identified several alternative pathways and interactions between different compartments (Shaw and Kundu 2015). The term 'alternative pathways' basically means the number of ways in which a cell can adjust its metabolism and tolerate a given perturbation in order to synthesize its required energy and biomass. This study has reported the usage of different alternative pathways as a result of reaction deletion. For example, phosphoglycerate kinase, which is a key enzyme of glycolysis, generates ATP from ADP along with the conversion of 1,3-bisphosphoglycerate to 3-phosphoglycertae. Shaw and Kundu (2015) have shown that deletion of this reaction increases the photon demand of the cell by 12.79%. The reason behind this is the readjustment of the cell to fulfil the ATP demand by utilizing other pathways to synthesize biomass. Another example of cellular adaptation in the cellulose biosynthesis pathway is by removing the enzyme phosphoglucomutase that converts glucose-6-phosphate to glucose-1-phosphate. This reaction is followed by the conversion of glucose-1-phosphate and UTP to UDP-glucose and pyrophosphate by the enzyme UDP-glucosepyrophosphorylase. It has been observed that in the absence of phosphoglucomutase, the cell utilizes another pathway for the production of cellulose and the photon demand increased by 6%. Another study (Poolman *et al*. 2009) on the model plant *Arabidopsis thaliana* has shown that when a low amount of ATP is needed for a cell, the ATP requirement can be fulfilled by a truncated TCA cycle, glycolysis, and ETC, and alternative modes of the TCA cycle come into play (Poolman *et al*. 2009).

Moreover, the results of the reaction deletion method (Shaw and Kundu 2015) show that deletion of different reactions in different cellular compartments can activate different biochemical modes in the cell. For example, the deletion of complexes I and V in mitochondria upregulates the malate–oxaloacetate shuttle in the chloroplast and the light-dependent cyclic reaction, and downregulates the light-dependent non-cyclic reaction. This causes variation in the ratio of ATP and NADPH, which are produced by the light-dependent cyclic and non-cyclic reactions. On the other hand, the effects of partial inhibition of a reaction within a metabolic network can be investigated by limiting the flux to a fraction of its wild-type value. A previous study (Chavali *et al*. 2008) has evaluated the effect of the presence of an inhibitor of a reaction by varying the flux through that reaction from its wild-type value to zero. Variations in growth rate have been observed with the variation in the flux of mitochondrial F_0F_1-ATP synthase. This study on the metabolic network also gives insight into the effect of gene deletion, with the identification of 69 single lethal gene deletions and 56 non-trivial lethal double-gene deletions (Chavali *et al*. 2008).

4.1.3 Incorporation of different omics data can mimic availability of metabolites and enzymes in a cell: A study (Shaw and Kundu 2013) on the genome-scale metabolic model of rice (*Oryza sativa*) investigated the effect of different transporters that transport metabolites from one compartment to another on the photon requirement for biomass synthesis and inter-compartmental interactions within a cell, depending on gene expression. They showed that the number of photons needed for biomass synthesis depends on the capacity of intra-cellular transporters. Different modes of the TCA cycle, cyclic or non-cyclic and different interactions between the compartments have also been analyzed in this study. For example, when sufficient amount of ATP is produced by chloroplastic light reactions, the over-production of ATP is prevented by truncating the TCA cycle and downregulating the ETC, whereas when alternative sources do not work, the TCA cycle operates in cyclic mode (Shaw and Kundu 2013). The effect of variations of different enzymatic gene expressions can further be analyzed in future using this method. Another study (Cheung *et al*. 2015) on a diel genome-scale model of *A. thaliana* leaf incorporated flux weighting factors to analyze the metabolic flexibility of a network. The cost-weighted FBA revealed several alternative modes of different pathways which were inactive when investigated using conventional FBA. For example, this study has shown the usage of different alternative pathways to dispose of the excess amount of reductants at different light intensities.

In a recent study (Maiti *et al*. 2023), FBA has been used to study a multi-segment model of a C_4 plant, *Setaria viridis*. They divided the leaf into four segments from the base, the most immature segment having the most proliferating cells, to the tip, the most immature segment having the most differentiated cells, including two growing segments in between. The different growth rates of each leaf segment of the plant were used as constraints, and transcriptomic data were incorporated in the objective function of the simulation. They observed metabolic variability in different segments of the leaf, and all the biomass components were not produced in each segment. Instead, different segments produced biomass components at different ratios and these components were exchanged according to the

need of the leaf segments. The requirement of carbon in a growing tip was fulfilled by the supply from the base of the leaf, whereas the mid-segments provided amino acids such as phenylalanine, glutamate, etc., to the base more than tip. Supply of the protein building blocks from the mid-segments reduces transport cost, as the mid-segments are closer to the base than the tip. Sucrose is the main transport element in the plant through phloem sap. It is observed that in a leaf, the plant prefers sucrose transport from the most mature segment, the tip. However, the dependencies of fatty acids are fulfilled from the neighboring cells (Maiti *et al*. 2023). A similar computational technique has been used in analyzing maize leaf metabolism at a multi-scale level (Bogart and Myers 2016).

4.1.4 Can we explain regulation of plant hormones by integrating omics data in metabolic network? It is known that different plant hormones are differentially produced under varied conditions at different parts of a plant. It is expected that the genes of their biosynthetic pathways may be co-regulated. For example, one can determine whether the genes involved in the biosynthetic pathway of hormones (say, auxin, gibberellin, etc.) are transcriptionally regulated by the same set of transcription factors. This can be achieved by integrating gene expression data and quantifying the co-occurrence of *cis*-regulatory elements present in a set of promoter sequences (Deb and Kundu 2015). Lakshmanan *et al*. (2015) integrated rice gene expression data under different light treatments with the rice metabolic network to unravel the transcriptional regulation of different phytohormone biosynthesis, to identify differentially regulating metabolic pathways (e.g., upregulation of photosynthesis and secondary metabolism in blue light) and also showed that upregulation of the abscisic acid (ABA) biosynthesis gene is related to the accumulation of ABA that can reduce ethylene biosynthesis inhibiting plant stem growth.

4.1.5 More realistic flux distribution patterns can be predicted by incorporating different constraints to mimic real scenarios in plants: Cheung *et al*. (2013) predicted a more accurate flux distribution by the incorporation of the energy cost for transportation of different molecules through plasma membranes and membranes of other organelles and the maintenance of cell. They incorporated the ATP requirement as a cost to the transporters of plasma membrane in order to import nutrients to the cell and the cost to the membranes of mitochondrion, peroxisome, and tonoplast as a cost of intracellular metabolite transport. The central metabolic pathways are not only involved in biomass production, but they also provide energy. And this energy is utilized for transporting ions, metabolites, and macromolecules and cell maintenance along with the synthesis of biomass. Thus, incorporating these costs to the model bring about noticeable changes in the flux distribution pattern of the central carbon metabolism. Simulation of this extended model predicted that 67% of the total energy is utilized for producing biomass and the remaining is used for cell maintenance. Glycolysis and the TCA cycle also give more accurate flux distributions, whereas no change of flux is observed in the case of the oxidative pentose phosphate pathway (OPPP). Addition of the ratio of fluxes through OPPP and the glycolysis pathway as another constraint gives more realistic results. They also analyzed the model for elevated temperature and hyperosmotic conditions. When temperature is increased, ATP and NADPH maintenance cost is increased and the carbon conversion coefficient decreases. However, in the case of hyperosmotic conditions, slow growth of *Arabidopsis* is observed due to restricted glucose uptake.

4.1.6 Interactions between light and dark metabolism can be captured during day–night cycles using FBA: Some analyses of leaf metabolism by FBA have been done on the models exposed to continuous light. In plants, there are different effects of day and night on leaves, and these effects should be incorporated into models in order to have more realistic flux distribution patterns for different objective functions. Cheung *et al*. (2014) have constructed a diel genome-scale model of *Arabidopsis* by applying constraints to a pre-existing model of *Arabiopsis* in such a way that metabolites produced during the day can be used for overnight cellular maintenance and metabolites stored at night can be used for different purposes. In this study, the two models of day and night phases were used as a single optimization problem. The day phase represents autotrophic metabolism where photon influx is allowed, whereas the night phase represents heterotrophic metabolism by restricting the value of photon flux to zero. They observed many differences in the two cases. For example, in the case of the diel model, starch synthesis was observed during the day to supply the carbon source for the night where no fixation of CO_2 is possible, while in the model continuously exposed to light, no starch synthesis is required as there is continuous assimilation of CO_2 occurring in the leaf. Another important difference is observed in the case of usage of citrate for glutamate and glutamine synthesis.

In the model with continuous light, citrate is synthesized in the peroxisome by citrate synthase and used in glutamate and glutamine synthesis. However, in the case of the diel model, citrate, synthesized by the mitochondrial TCA cycle at night, is stored in the vacuole and used further for the production of 2-oxoglutarate followed by the production of glutamate synthesis. They also predicted that in a similar way, nitrate is imported to the vacuole from the xylem during the night, and it leaves the vacuole during daytime and is utilized in producing amino acids, which are then released into the phloem during the night. In the light phase, the photosynthetic electron transport pathways and the Calvin–Benson cycle have maximum fluxes through them for the synthesis of sucrose, starch, and amino acids, and the TCA cycle is operated in a non-cyclic fashion. However, in the dark phase, starch is degraded to provide carbon to the cell and large fluxes are observed through glycolysis, OPPP, the TCA cycle, and mitochondrial ETC. In this phase, the TCA is operated in full cyclic mode.

In another study (Tan and Cheung 2020), stomatal opening and closing due to variation in the metabolism of guard cells of C_3 plants during day and night have been analyzed. The authors constructed a model consisting of four phases: opening of stomata at the time of sunrise (1 h), daytime (11 h), closure of stomata at the time of sunset (1 h), and nighttime (11 h). In the four phases all the reactions are same, whereas different constraints are applied depending on the phases. They have observed that in the open phases, K^+ and malate are accumulated through the import by the K^+/H^+ symporter and degradation of starch stored at night, respectively. The conversion of the Calvin–Benson cycle products to phospoenolpyruvate (PEP) by glycolysis and then conversion of PEP to first OAA and then malate is another way in which malate is accumulated. Accumulation of osmolytes and ions is responsible for the opening of stomata in this phase. In the day phase, sucrose is imported for the maintenance of stomatal opening and K^+ is exported outside the guard cell. This large amount of sucrose is produced from degradation of malate and the rest is provided by the Calvin–Benson cycle. In the closed phase, sucrose is degraded, and hexose phosphate is produced. This hexose phosphate is used in starch synthesis and production of NADPH through OPPP and ATP through the TCA cycle and mitochondrial ETC. In the night phase, the starch produced in the closed phase is used for the production of ATP and NADPH in order to maintain the metabolism of the guard cell. The remaining starch in the night phase is utilized as a source of malate during the open phase for stomatal opening (Tan and Cheung 2020).

4.1.7 Can we investigate the effect of different intensities of light on cellular metabolism? Poolman *et al.* (2013) simulated a model of the rice plant with different photon values using FBA and analyzed the results. In this study, it was shown that in low light, ATP is generated by mitochondria in association with oxidation of pyruvate and malate and decreases as light intensity increases. At high light intensity, the model shifts from using cytochrome oxidase to alternative oxidase in mitochondria to protect the plant against harmful effects of excess light (Bartoli *et al.* 2005). Results also shows that photorespiration increases as photon flux increases, and at high light level, photorespiration is fully active to dissipate the effect of excess energy. The same result has been observed in another study (Chatterjee *et al.* 2017).

4.1.8 Explaining how redox is balanced in a cell in different levels of photorespiration: Chatterjee *et al.* (2017) further showed that with increased photorespiration, to meet the requirement of NADH for peroxisomal hydroxy pyruvate reductase (HPR1), different combinations of reactions and transporters are involved in different levels of photorespiration and the cellular energy demand is maintained. As photorespiration increases, the import of malate to mitochondria decreases, and it stops at medium light. As light increases, to supply more NADH to the peroxisome, mitochondrial malate dehydrogenase works in the opposite direction and produces malate. When light is further increased, chloroplastic triose phosphate exchange involving glyceraldehyde-3-phosphate (GAP) and 3-phosphoglycerate (PGA) comes into play. They make available chloroplastic NADH and ATP in the cytosol and supply that NADH to the peroxisome to fulfil the reductant demand of HPR1. In this manner, the dynamic interplay between the four compartments mitochondrion, chloroplast, cytosol, and peroxisome has been observed in order to dissipate the effect of high light through photorespiration. Further, it is analyzed that pyruvate dehydrogenase in mitochondria gets inactivated by light (Poolman *et al.* 2013). This light scanning can be done for analyzing the activity of other enzymes of metabolic pathways in the presence and absence of light.

4.1.9 Can we study the effect of nutrient availability and other factors on metabolism? Refinement of the results of FBA can be done by incorporating

thermodynamic and biological information of the reactions of the model as constraints. These additional constraints allow the usage of proteomics and metabolomics data along with FBA. The thermodynamic link between flux directions and metabolite concentrations is incorporated in the model in such a way that reaction directionality is always consistent with measured metabolite concentrations and the Gibbs free energy for the reaction (Hoppe *et al*. 2007). On the other hand, the concentrations of the catalyzing enzymes in the network, represented by weighting coefficients, are used as a set of constraints to the model (De *et al*. 2008).

The availability of nutrients (such as nitrogen, oxygen, etc.) in the environment also affects the system. Previous studies have shown that maximum cell growth rates under different environmental conditions, such as aerobic or anaerobic environments, various carbon sources, ammonium, or nitrate as nitrogen source, etc., can be accurately predicted using FBA (Varma and Palsson 1994; Mahadevan and Schilling 2003). For example, the maximum growth rate for *E. coli* on glucose under aerobic conditions predicted by FBA coincides with the experimentally observed growth rates for adaptively evolved *E. coli* strains (Long *et al*. 2017), and acetate is secreted as a metabolic by-product at high growth rates, as observed in experimental studies (Varma and Palsson 1994; Mahadevan and Schilling 2003). The maximum rates of nutrient uptake limit the maximum growth rate of the system (Varma and Palsson 1994). Another study examined the growth of the system on glucose and succinate due to changes in the internal conditions of the network (such as the removal of a reaction) and environmental conditions (such as the availability of substrate and oxygen) using a combined application of pathway analysis and flux balance analysis (Schilling *et al*. 2000).

4.1.10 Metabolic interactions in a symbiotic relationship between bacteria and plants: An interesting study was performed by Pfau *et al*. (2018) to understand the metabolic interactions between nitrogen-fixing microorganisms and plants. They took the genome-scale model of the plant *Medicago truncatula* as a model for legumes and linked the model with a model of *Sinorhizobium meliloti* as the symbiont. The results of FBA showed that the growth of the plant in the presence of its symbiont is reduced as it needs to supply carbon sources to the symbiont. There is growth of the plant even in low levels of nitrogen because of sufficient supply from the symbiont. They have further observed that, since oxidative phosphorylation provides most of the energy required for the fixation of nitrogen by nitrogenase enzyme in bacteroids, the concentration of oxygen is an important factor in controlling nitrogen fixation. A large amount of O_2 irreversibly inhibits the nitrogenase complex. The amount of oxygen present is maintained by the plant by leghemoglobin (Pfau *et al*. 2018).

4.2 *Usage of elementary flux mode analysis (EFMA) for determining various modes of metabolism*

The EFMA method was used in a previous study to investigate photorespiration and its interactions with other mitochondrial metabolisms and ATP synthesis (Huma *et al*. 2018). The authors constructed a model consisting of four compartments: mitochondrion, chloroplast, peroxisome, and cytosol. After simulating the model, they identified 43 essential reactions out of the 74 reactions active in at least one elementary flux mode (EFM), and 56 EFMs have been obtained in the cellular model of C_3 plant metabolism that represent all feasible routes of photorespiration. They classified the EFMs into four major groups. Different combinations of modes are active in different circumstances, depending on the environmental conditions and other factors. For example, in some energy-dissipating modes, they observed that mitochondrial malate dehydrogenase (MalDH) operates in the reverse direction producing oxaloacetate from malate which is produced in and transported from the chloroplast, cytosol, and/or peroxisome. This is called an energy-dissipating mode, as it oxidizes excess NADH. In these modes, excess photons are absorbed by photorespiration, but have no effect on cellular metabolism. In short, these modes are active to protect the photosystem from getting inhibited by excess light, which is called photoinhibition. In some EFMs, MalDH is active in the forward direction, producing malate and excess NADH. In these modes, ATP is generated by both cyclic and non-cyclic photophosphorylations. When cyclic photophosphorylation is limited, to meet the cell's ATP demand, non-cyclic photophosphorylation produces ATP in such a manner that excess NADPH is produced. However, in EFMs in which mitochondrial MalDH is inactive, excess amount of reductants is produced by the non-cyclic light reaction in order to maintain photorespiration and the evolution of a net amount of O_2 is observed. Photorespiration gets coupled with nitrogen assimilation and the glutathione

ascorbate cycle to reoxidize this excess amount of reduction. One of the major findings is that the assimilation quotient, i.e., the amount of CO_2 fixed per O_2 released, does not change with photorespiration unless nitrogen assimilation is associated with it.

Another study (Rohwer and Botha 2001) using elementary mode analysis (EMA) revealed 14 elementary modes in the central carbon metabolism and sucrose accumulation in sugarcane. Flux modes leading from extracellular glucose or fructose to vacuolar sucrose accumulation, leading from extracellular glucose or fructose to glycolysis and respiration, and a set of five futile cycles have been identified in this study (Rohwer and Botha 2001). EMA can also be expanded by introducing the power-law formula into EMA in order to link an enzyme activity profile to a metabolic flux distribution. A method called enzyme control flux (ECF) successfully predicts the changes in flux distribution due to a change in an enzyme profile in *E. coli* and *B. subtilis* (Kurata *et al*. 2007). Thus, we can expect that regulation of mitochondrial metabolism (described earlier) in different environmental, enzymatic, and stressed conditions can be examined using EMA.

5. Challenges

In this review, we have focused on some computational approaches like FBA and EFMA and discussed how they have been used in previous studies to investigate the metabolism of mitochondria, its regulations, and its interactions with other organelles. We have also discussed how over-represented *cis*-regulatory interactions can be integrated to find potential co-regulation of plant hormones. Below, we briefly discuss a few computational tools which can be used to obtain greater insight into plant metabolism and its interactions.

To analyze different regulations, previous studies have shown that expression data can be incorporated in FBA in two ways: by directly using them to constrain flux through specific reactions in the model or adding various mathematical rules to the model. In the first approach, one can set the fluxes of reactions to zero if their expressions are low, and if they have high expression values, then that value is set to be the upper bound of the particular reaction (Åkesson *et al*. 2004; Becker and Palsson 2008; Shlomi *et al*. 2008; Colijn *et al*. 2009; van Berlo *et al*. 2009; Jerby *et al*. 2010; Jensen and Papin 2011; Maiti *et al*. 2023). In the second approach, different mathematical modifications of FBA have been effected to incorporate expression data (Covert *et al*. 2004, 2008; Shlomi *et al*. 2007; Lee *et al*. 2008).

One of such modifications is known as regulatory flux balance analysis (rFBA), which requires Boolean rules that represent transcriptomic data to be applied over an existing stoichiometric model of metabolism (Covert *et al*. 2001; Covert and Palsson 2002, 2003). The 'ON' and 'OFF' states of the gene products (such as proteins) are defined by the Boolean rules to constrain the flux through the corresponding reactions catalyzed by them in the metabolism. For example, in a particular environmental condition, the flux of a reaction catalyzed by a gene product is set to zero if the transcription of the particular gene is turned 'OFF'. Several studies of rFBA on stoichiometric models of *E. coli* and *S. cerevisiae* metabolisms showed consistency with experimental measurements (Covert and Palsson 2003; Herrgård *et al*. 2006). For example, in a study on genome-scale metabolism of *E. coli*, FBA without gene regulatory constraints shows only 86% agreement with experimental results, while rFBA shows 91% agreement (Covert *et al*. 2001; Covert and Palsson 2003).

To overcome the restriction of application of expression data in a binary manner, another approach called probabilistic regulation of metabolism (PROM) has been developed to apply continuous flux restrictions based on gene expression data. This method shows 95% accuracy in *E. coli* and *Mycobacterium tuberculosis* metabolisms (Chandrasekaran and Price 2010).

Transcriptionally controlled flux balance analysis (tFBA) (van Berlo *et al*. 2009) is another extension of FBA to regulate flux through a reaction if the expression of the associated gene changes significantly from one condition to another.

Furthermore, parsimonious flux balance analysis (pFBA) maximizes biomass yield and minimizes total flux through a network instead of using expression data (Lewis *et al*. 2010). Linear bound FBA (LBFBA) gives greater accuracy than pFBA in predicting fluxes by using expression data. Other expression-based methods that incorporate transcriptomic data have been reviewed in a previous study (Machado and Herrgård 2014). Thus, it is possible to use this vast field of FBA to analyze metabolic and genetic regulations (described earlier) of mitochondrial metabolism.

Furthermore, three stoichiometric models of *H. pylori*, *E. coli*, and *S. cerevisiae* have been analyzed using flux coupling finder (FCF) to provide a detailed analysis of the coupling of their reactions (Burgard *et al*. 2004). The result showed that 10%, 14%, and

29% of their respective reactions were blocked unconditionally. Moreover, they found that the percentage of blocked reactions depends on the size of the network: the larger the network, the higher is the percentage of blocked reactions. Furthermore, it can be concluded that larger models of *E. coli* and *S. cerevisiae* have greater flexibility and redundancy, since the percentage of reactions in coupled sets decreases substantially with model size. Anaerobic conditions also have little impact on the coupling of reactions (Burgard *et al*. 2004). Similar analysis can be done for the models of different plant species in order to investigate the coupling of reactions in different cellular conditions.

Proper implementation of the above-mentioned tools will help us to further analyze (i) the metabolic interactions by regulating the TCA cycle and other metabolic pathways of plants by incorporating different omics data to the model, (ii) more realistic results by incorporating the enzymatic costs of reactions and different constraints to mimic the different cellular conditions of plants, (iii) how robust a plant system is to maintain its overall metabolism and redox when different cells produce different biomass depending on the availability of light and nutrients, (iv) the change in metabolic interactions with the change in pH, i.e., concentration of H^+ in the cell, and (v) the coupling of different reactions, i.e., how change in one reaction affects the other reactions of the metabolic pathways of plants using FCF.

Although several computational studies shed light on plant metabolism, its variations and regulations, a large number of cellular events like change in enzymatic activities, interactions of cellular metabolism with signaling pathways, and differential growths of different parts of a plant and its metabolic variations are unexplained even today.

References

Affourtit C, Krab K, Leach GR, *et al*. 2001 New insights into the regulation of plant succinate dehydrogenase: on the role of the protonmotive force. *J. Biol. Chem.* **276** 32567–32574

Åkesson M, Förster J and Nielsen J 2004 Integration of gene expression data into genome-scale metabolic models. *Metab. Eng.* **6** 285–293

Alejandre M, Segovia J, Zafra M, *et al*. 1979 Characteristics of citrate synthase from *Agave americana L.* leaves. *Z. Pflanzenphysiol.* **94** 85–93

Araujo WL, Nunes-Nesi A, Nikoloski Z, *et al*. 2012 Metabolic control and regulation of the tricarboxylic acid cycle in photosynthetic and heterotrophic plant tissues. *Plant Cell Environ.* **35** 1–21

Armstrong AF, Badger MR, Day DA, *et al*. 2008 Dynamic changes in the mitochondrial electron transport chain underpinning cold acclimation of leaf respiration. *Plant Cell Environ.* **31** 1156–1169

Arnon DI 1971 The light reactions of photosynthesis. *Proc. Natl. Acad. Sci. USA* **68** 2883–2892

Barbareschi D, Longo GP, Servettaz O, *et al*. 1974 Citrate synthetase in mitochondria and glyoxysomes of maize scutellum. *Plant Physiol.* **53** 802–807

Bartoli CG, Gomez F, Gergoff G, *et al*. 2005 Up-regulation of the mitochondrial alternative oxidase pathway enhances photosynthetic electron transport under drought conditions. *J. Exp. Bot.* **56** 1269–1276

Becker SA and Palsson BO 2008 Context-specific metabolic networks are consistent with experiments. *PLoS Comput. Biol.* **4** e1000082

Behal RH and Oliver DJ 1997 Biochemical and molecular characterization of fumarase from plants: purification and characterization of the enzyme-cloning, sequencing, and expression of the gene. *Arch. Biochem. Biophys.* **348** 65–74

Bocobza SE, Malitsky S, Araújo WL, *et al*. 2013 Orchestration of thiamin biosynthesis and central metabolism by combined action of the thiamin pyrophosphate riboswitch and the circadian clock in *Arabidopsis*. *Plant Cell* **25** 288–307

Bogart E and Myers CR 2016 Multiscale metabolic modeling of C4 plants: connecting nonlinear genome-scale models to leaf-scale metabolism in developing maize leaves. *PLoS One* **11** e0151722

Bourguignon J, Neuburger M and Douce R 1988 Resolution and characterization of the glycinecleavage reaction in pea leaf mitochondria. Properties of the forward reaction catalysed by glycine decarboxylase and serine hydroxymethyltransferase. *Biochem. J.* **255** 169–178

Burgard AP, Nikolaev EV, Schilling CH, *et al*. 2004 Flux coupling analysis of genome scale metabolic network reconstructions. *Genome Res.* **14** 301–312

Bunik VI and Fernie AR 2009 Metabolic control exerted by the 2-oxoglutarate dehydrogenase reaction: a cross-kingdom comparison of the crossroad between energy production and nitrogen assimilation. *Biochem. J.* **422** 405–421

Campbell C, Atkinson L, Zaragoza-Castells J, *et al*. 2007 Acclimation of photosynthesis and respiration is asynchronous in response to changes in temperature regardless of plant functional group. *New Phytol.* **176** 375–389

Chandrasekaran S and Price ND 2010 Probabilistic integrative modeling of genome-scale metabolic and regulatory networks in *Escherichia coli* and mycobacterium tuberculosis. *Proc. Natl. Acad. Sci. USA* **107** 17845–17850

Chatterjee A, Huma B, Shaw R, *et al*. 2017 Reconstruction of *Oryza sativa indica* genome scale metabolic model and its responses to varying RuBisCO activity, light intensity, and enzymatic cost conditions. *Front. Plant Sci.* **8** 2060

Chavali AK, Whittemore JD, Eddy JA, *et al*. 2008 Systems analysis of metabolism in the pathogenic trypanosomatid *Leishmania major*. *Mol. Syst. Biol.* **4** 177

Cheung CM, Poolman MG, Fell DA, *et al*. 2014 A diel flux balance model captures interactions between light and dark metabolism during day-night cycles in c3 and crassulacean acid metabolism leaves. *Plant Physiol.* **165** 917–929

Cheung CM, Ratcliffe RG and Sweetlove LJ 2015 A method of accounting for enzyme costs in flux balance analysis reveals alternative pathways and metabolite stores in an illuminated *Arabidopsis* leaf. *Plant Physiol.* **169** 1671–1682

Cheung CM, Williams TC, Poolman MG, *et al*. 2013 A method for accounting for maintenance costs in flux balance analysis improves the prediction of plant cell metabolic phenotypes under stress conditions. *Plant J.* **75** 1050–1061

Colijn C, Brandes A, Zucker J, *et al*. 2009 Interpreting expression data with metabolic flux models: predicting *Mycobacterium tuberculosis* mycolic acid production. *PLoS Comput. Biol.* **5** e1000489

Cooper CE and Brown GC 2008 The inhibition of mitochondrial cytochrome oxidase by the gases carbon monoxide, nitric oxide, hydrogen cyanide and hydrogen sulfide: chemical mechanism and physiological significance. *J. Bioenerg. Biomembr.* **40** 533–539

Covert MW, Knight EM, Reed JL, *et al*. 2004 Integrating highthroughput and computational data elucidates bacterial networks. *Nature* **429** 92–96

Covert MW and Palsson BØ 2002 Transcriptional regulation in constraints-based metabolic models of *Escherichia coli* *210. *J. Biol. Chem.* **277** 28058–28064

Covert MW and Palsson BØ 2003 Constraints-based models: regulation of gene expression reduces the steady-state solution space. *J. Theor. Biol.* **221** 309–325

Covert MW, Xiao N, Chen TJ, *et al*. 2008 Integrating metabolic, transcriptional regulatory and signal transduction models in *Escherichia coli*. *Bioinformatics* **24** 2044–2050

Covert MW, Schilling CH and Palsson BØ 2001 Regulation of gene expression in flux balance models of metabolism. *J. Theor. Biol.* **213** 73–88

Cox G and Davies D 1969 The effects of pH and citrate on the activity of nicotinamide–adenine dinucleotide-specific isocitrate dehydrogenase from pea mitochondria. *Biochem. J.* **113** 813–820

da Fonseca-Pereira P, Souza PV, Hou LY, *et al*. 2020 Thioredoxin h2 contributes to the redox regulation of mitochondrial photorespiratory metabolism. *Plant Cell Environ.* **43** 188–208

Daloso DM, Müller K, Obata T, *et al*. 2015 Thioredoxin, a master regulator of the tricarboxylic acid cycle in plant mitochondria. *Proc. Natl. Acad. Sci. USA* **112** E1392–E1400

De RK, Das M and Mukhopadhyay S 2008 Incorporation of enzyme concentrations into fba and identification of optimal metabolic pathways. *BMC Syst. Biol.* **2** 1–16

de Oliveira Dal'Molin CG, Quek LE, Palfreyman RW, *et al*. 2010 AraGEM, a genome-scale reconstruction of the primary metabolic network in *Arabidopsis*. *Plant Physiol.* **152** 579–589

de Oliveira Dal'Molin CG, Quek LE, Palfreyman RW, *et al*. 2010 C4GEM, a genome-scale metabolic model to study c4 plant metabolism. *Plant Physiol.* **154**, 1871–1885

Deb A and Kundu S 2015 Deciphering cis-regulatory element mediated combinatorial regulation in rice under blast infected condition. *PLoS One* **10** e0137295

Ederli L, Morettini R, Borgogni A, *et al*. 2006 Interaction between nitric oxide and ethylene in the induction of alternative oxidase in ozone-treated tobacco plants. *Plant Physiol.* **142** 595–608

Eprintsev AT, Fedorin DN, Nikitina MV, *et al*. 2015 Expression and properties of the mitochondrial and cytosolic forms of aconitase in maize scutellum. *J. Plant Physiol.* **181** 14–19

Eprintsev AT, Fedorin DN, Sazonova OV, *et al*. 2018 Expression and properties of the mitochondrial and cytosolic forms of fumarase in sunflower cotyledons. *Plant Physiol. Biochem.* **129** 305–309

Fiorani F, Umbach AL and Siedow JN 2005 The alternative oxidase of plant mitochondria is involved in the acclimation of shoot growth at low temperature. A study of *Arabidopsis* AOX1a transgenic plants. *Plant Physiol.* **139** 1795–1805

Flügel F, Timm S, Arrivault S, *et al*. 2017 The photorespiratory metabolite 2-phosphoglycolate regulates photosynthesis and starch accumulation in *Arabidopsis*. *Plant Cell* **29** 2537–2551

Gupta KJ, Shah JK, Brotman Y, *et al*. 2012 Inhibition of aconitase by nitric oxide leads to induction of the alternative oxidase and to a shift of metabolism towards biosynthesis of amino acids. *J. Exp. Bot.* **63** 1773–1784

Hanning I, Baumgarten K, Schott K, *et al*. 1999 Oxaloacetate transport into plant mitochondria. *Plant Physiol.* **119** 1025–1032

Herrgård MJ, Lee BS, Portnoy V, *et al*. 2006 Integrated analysis of regulatory and metabolic networks reveals novel regulatory mechanisms in *Saccharomyces cerevisiae*. *Genome Res.* **16** 627–635

Hodges M, Flesch V, Gálvez S, *et al*. 2003 Higher plant NADP+-dependent isocitrate dehydrogenases, ammonium assimilation and NADPH production. *Plant Physiol. Biochem.* **41** 577–585

Hoppe A, Hoffmann S and Holzhütter HG 2007 Including metabolite concentrations into flux balance analysis:

thermodynamic realizability as a constraint on flux distributions in metabolic networks. *BMC Syst. Biol.* **1** 1–12

Huang W, Hu H and Zhang SB 2015 Photorespiration plays an important role in the regulation of photosynthetic electron flow under fluctuating light in tobacco plants grown under full sunlight. *Front. Plant Sci.* **6** 621

Huma B, Kundu S, Poolman MG, *et al*. 2018 Stoichiometric analysis of the energetics and metabolic impact of photorespiration in c3 plants. *Plant J.* **96** 1228–1241

Igamberdiev AU and Gardeström P 2003 Regulation of NAD-and NADP-dependent isocitrate dehydrogenases by reduction levels of pyridine nucleotides in mitochondria and cytosol of pea leaves. *Biochim. Biophys. Acta* **1606** 117–125

Jacoby RP, Li L, Huang S, *et al*. 2012 Mitochondrial composition, function, and stress response in plants. *J. Integr. Plant Biol.* **54** 887–906

Jensen PA and Papin JA 2011 Functional integration of a metabolic network model and expression data without arbitrary thresholding. *Bioinformatics* **27** 541–547

Jerby L, Shlomi T and Ruppin E 2010 Computational reconstruction of tissue-specific metabolic models: application to human liver metabolism. *Mol. Syst. Biol.* **6** 401

Kurata H, Zhao Q, Okuda R, *et al*. 2007 Integration of enzyme activities into metabolic flux distributions by elementary mode analysis. *BMC Syst. Biol.* **1** 1–14

Lakshmanan M, Lim SH, Mohanty B, *et al*. 2015 Unraveling the light-specific metabolic and regulatory signatures of rice through combined in silico modeling and multiomics analysis. *Plant Physiol.* **169** 3002–3020

Lancien M, Gadal P and Hodges M 1998 Molecular characterization of higher plant NAD-dependent isocitrate dehydrogenase: evidence for a heteromeric structure by the complementation of yeast mutants. *Plant J.* **16** 325–333

Le XH, Lee CP, Monachello D, *et al*. 2022 Metabolic evidence for distinct pyruvate pools inside plant mitochondria. *Nat. Plants* **8** 694–705

Leegood RC, Lea PJ, Adcock MD, *et al*. 1995 The regulation and control of photorespiration. *J. Exp. Bot.* 1397–1414

Lee JM, Gianchandani EP, Eddy JA, *et al*. 2008 Dynamic analysis of integrated signaling, metabolic, and regulatory networks. *PLoS Comput. Biol.* **4** e1000086

Lewis NE, Hixson KK, Conrad TM, *et al*. 2010 Omic data from evolved *E. coli* are consistent with computed optimal growth from genome-scale models. *Mol. Syst. Biol.* **6** 390

Long CP, Gonzalez JE, Feist AM, *et al*. 2017 Fast growth phenotype of *E. coli* k-12 from adaptive laboratory evolution does not require intracellular flux rewiring. *Metab. Eng.* **44** 100–107

Lotz K, Hartmann A, Grafahrend-Belau E, *et al*. 2014 Elementary flux modes, flux balance analysis, and their application to plant metabolism. *Methods Mol. Biol.* **1083** 231–252

Machado D and Herrgård M 2014 Systematic evaluation of methods for integration of transcriptomic data into constraint-based models of metabolism. *PLoS Comput. Biol.* **10** e1003580

Mahadevan R and Schilling CH 2003 The effects of alternate optimal solutions in constraint-based genome-scale metabolic models. *Metab. Eng.* **5** 264–276

Maiti R, Shaw R, Cheung CM, *et al*. 2023 Metabolic modelling revealed metabolic interactions between four segments of Setaria viridis leaves. *J. Biosci.* **48** 26

McIntosh CA and Oliver DJ 1992 NAD+-linked isocitrate dehydrogenase: isolation, purification, and characterization of the protein from pea mitochondria. *Plant Physiol.* **100** 69–75

Millar AH, Whelan J, Soole KL, *et al*. 2011 Organization and regulation of mitochondrial respiration in plants. *Annu. Rev. Plant Biol.* **62** 79–104

Mintz-Oron S, Meir S, Malitsky S, *et al*. 2012 Reconstruction of *Arabidopsis* metabolic network models accounting for subcellular compartmentalization and tissue specificity. *Proc. Natl. Acad. Sci. USA* **109** 339–344

Moore AL and Siedow JN 1991 The regulation and nature of the cyanide-resistant alternative oxidase of plant mitochondria. *Biochim. Biophys. Acta* **1059** 121–140

Moore AL, Umbach AL and Siedow JN 1995 Structure-function relationships of the alternative oxidase of plant mitochondria: a model of the active site. *J. Bioenerg. Biomembr.* **27** 367–377

Moreira TB, Shaw R, Luo X, *et al*. 2019 A genome-scale metabolic model of soybean (*Glycine max*) highlights metabolic fluxes in seedlings. *Plant Physiol.* **180** 1912–1929

Morgan MJ, Lehmann M, Schwarzlander M, *et al*. 2008 Decrease in manganese superoxide dismutase leads to reduced root growth and affects tricarboxylic acid cycle flux and mitochondrial redox homeostasis. *Plant Physiol.* **147** 101–114

Neuburger M, Bourguignon J and Douce R 1986 Isolation of a large complex from the matrix of pea leaf mitochondria involved in the rapid transformation of glycine into serine. *FEBS Lett.* **207** 18–22

Nishio K and Mizushima T 2020 Structural and biochemical characterization of mitochondrial citrate synthase 4 from *Arabidopsis thaliana*. *Acta Crystallogr. F Struct. Biol. Commun.* **76** 109–115

Nunes-Nesi A, Araújo WL, Obata T, *et al*. 2013 Regulation of the mitochondrial tricarboxylic acid cycle. *Curr. Opin. Plant Biol.* **16** 335–343

Ogren WL 1984 Photorespiration: pathways, regulation, and modification. *Ann. Rev. Plant Physiol.* **35** 415–442

Oikawa K, Hayashi M, Hayashi Y, *et al*. 2019 Re-evaluation of physical interaction between plant peroxisomes and other organelles using live-cell imaging techniques. *J. Integr. Plant Biol.* **61** 836–852

Orth JD, Thiele I and Palsson BØ 2010 What is flux balance analysis? *Nat. Biotechnol.* **28** 245–248

Palmer J and Wedding R 1966 Purification and properties of succinyl-CoA synthetase from jerusalem artichoke mitochondria. *Biochim. Biophys. Acta.* **113** 167–174

Pastore D, Trono D, Laus MN, *et al*. 2001 Alternative oxidase in durum wheat mitochondria. activation by pyruvate, hydroxypyruvate and glyoxylate and physiological role. *Plant Cell Physiol.* **42** 1373–1382

Pfau T, Christian N, Masakapalli SK, *et al*. 2018 The intertwined metabolism during symbiotic nitrogen fixation elucidated by metabolic modelling. *Sci. Rep.* **8** 12504

Poolman MG, Kundu S, Shaw R, *et al*. 2013 Responses to light intensity in a genome-scale model of rice metabolism. *Plant Physiol.* **162** 1060–1072

Poolman MG, Miguet L, Sweetlove LJ, *et al*. 2009 A genome-scale metabolic model of *Arabidopsis* and some of its properties. *Plant Physiol.* **151** 1570–1581

Popova TN and de Carvalho MAAP 1998 Citrate and isocitrate in plant metabolism. *Biochim. Biophys. Acta* **1364** 307–325

Reinholdt O, Bauwe H, Hagemann M, *et al*. 2019 Redox-regulation of mitochondrial metabolism through thioredoxin o1 facilitates light induction of photosynthesis. *Plant Signal. Behav.* **14** 1674607

Rohwer JM 2012 Kinetic modelling of plant metabolic pathways. *J. Exp. Bot.* **63** 2275–2292

Rhoads DM and Subbaiah CC 2007 Mitochondrial retrograde regulation in plants. *Mitochondrion* **7** 177–194

Ribas-Carbo M, Aroca R, Gonzalez-Meler MA, *et al*. 2000 The electron partitioning between the cytochrome and alternative respiratory pathways during chilling recovery in two cultivars of maize differing in chilling sensitivity. *Plant Physiol.* **122** 199–204

Rohwer JM and Botha FC 2001 Analysis of sucrose accumulation in the sugar cane culm on the basis of in vitro kinetic data. *Biochem. J.* **358** 437–445

Rustin P, Moreau F and Lance C 1980 Malate oxidation in plant mitochondria via malic enzyme and the cyanide-insensitive electron transport pathway. *Plant Physiol.* **66** 457–462

Saha B, Borovskii G and Panda SK 2016 Alternative oxidase and plant stress tolerance. *Plant Signal. Behav.* **11** e1256530

Saha R, Suthers PF and Maranas CD 2011 Zea mays iRS1563: a comprehensive genome-scale metabolic reconstruction of maize metabolism. *PLoS One* **6** e21784

Schuster S and Fell D 2007 Modeling and simulating metabolic networks; in *Bioinformatics – From genomes to therapies* (Ed.) T Lengauer (Weinheim: Wiley-VCH) pp 755–805

Seelert H and Dencher NA 2011 ATP synthase superassemblies in animals and plants: two or more are better. *Biochim. Biophys. Acta* **1807** 1185–1197

Schilling CH, Edwards JS, Letscher D, *et al*. 2000 Combining pathway analysis with flux balance analysis for the comprehensive study of metabolic systems. *Biotechnol. Bioeng.* **71** 286–306

Schmidtmann E, König AC, Orwat A, *et al*. 2014 Redox regulation of *Arabidopsis* mitochondrial citrate synthase. *Mol Plant.* **7** 156–169

Schuster S, Dandekar T and Fell DA 1999 Detection of elementary flux modes in biochemical networks: a promising tool for pathway analysis and metabolic engineering. *Trends Biotechnol.* **17** 53–60

Searle SY, Thomas S, Griffin KL, *et al*. 2011 Leaf respiration and alternative oxidase in field-grown alpine grasses respond to natural changes in temperature and light. *New Phytol.* **189** 1027–1039

Sharkey TD 2023 The discovery of rubisco. *J. Exp. Bot.* **74** 510–519

Shaw R and Cheung CM 2019 A mass and charge balanced metabolic model of setaria viridis revealed mechanisms of proton balancing in c4 plants. *BMC Bioinform.* **20** 1–11

Shaw R and Kundu S 2013 Random weighting through linear programming into intracellular transporters of rice metabolic network; in *Pattern recognition and machine intelligence* (Eds.) P Maji, A Ghosh, MN Murty, *et al.* (Berlin: Springer) pp. 662–728

Shaw R and Kundu S 2015 Metabolic plasticity and inter-compartmental interactions in rice metabolism: an analysis from reaction deletion study. *PLoS One* **10** e0133899

Shlomi T, Cabili MN, Herrgård MJ, *et al*. 2008 Network-based prediction of human tissue-specific metabolism. *Nat. Biotechnol.* **26** 1003–1010

Shlomi T, Eisenberg Y, Sharan R, *et al*. 2007 A genome-scale computational study of the interplay between transcriptional regulation and metabolism. *Mol. Syst. Biol.* **3** 101

Shi K, Fu LJ, Zhang S, *et al*. 2013 Flexible change and cooperation between mitochondrial electron transport and cytosolic glycolysis as the basis for chilling tolerance in tomato plants. *Planta* **237** 589–601

Siedow JN and Day DA 2000 Respiration and photorespiration; in *Biochemistry and molecular biology of plants* 1st edition (Eds.) BB Buchanan, W Gruissem and RL Jones (Rockville, MD: American Soceity of Plant Physiologists) pp 676–728

Simonin V and Galina A 2013 Nitric oxide inhibits succinate dehydrogenase-driven oxygen consumption in potato tuber mitochondria in an oxygen tension-independent manner. *Biochem. J.* **449** 263–273

Sipari N, Lihavainen J, Shapiguzov A, *et al*. 2020 Primary metabolite responses to oxidative stress in early-senescing and paraquat resistant *Arabidopsis thaliana* rcd1 (radical-induced cell death 1). *Front. Plant Sci.* **11** 194

Sluse F and Jarmuszkiewicz W 1998 Alternative oxidase in the branched mitochondrial respiratory network: an

overview on structure, function, regulation, and role. *Braz. J. Med. Biol. Res.* **31** 733–747

Stevens FJ, Dong Li A, Salman Lateef S, *et al*. 1997 Identification of potential interdomain disulfides in three higher plant mitochondrial citrate synthases: paradoxical differences in redox-sensitivity as compared with the animal enzyme. *Photosynth. Res.* **54** 185–197

Strumilo S 2005 Short-term regulation of the α-ketoglutarate dehydrogenase complex by energylinked and some other effectors. *Biochemistry* **70** 726–729

Studart-Guimarães C, Gibon Y, Frankel N, *et al*. 2005 Identification and characterisation of the α and β subunits of succinyl CoA ligase of tomato. *Plant Mol. Biol.* **59** 781–791

Sweetlove LJ, Beard KF, Nunes-Nesi A, *et al*. 2010 Not just a circle: flux modes in the plant TCA cycle. *Trends Plant Sci.* **15** 462–470

Tan XJ and Cheung CM 2020 A multiphase flux balance model reveals flexibility of central carbon metabolism in guard cells of c3 plants. *Plant J.* **104** 1648–1656

Timm S, Florian A, Arrivault S, *et al*. 2012 Glycine decarboxylase controls photosynthesis and plant growth. *FEBS Lett.* **586** 3692–3697

Timm S and Hagemann M 2020 Photorespiration—how is it regulated and how does it regulate overall plant metabolism? *J. Exp. Bot.* **71** 3955–3965

Tovar-Méndez A, Miernyk JA and Randall DD 2003 Regulation of pyruvate dehydrogenase complex activity in plant cells. *Eur. J. Biochem.* **270** 1043–1049

Tretter L and Adam-Vizi V 2000 Inhibition of krebs cycle enzymes by hydrogen peroxide: a key role of α-ketoglutarate dehydrogenase in limiting nadh production under oxidative stress. *J. Neurosci.* **20** 8972–8979

Umbach AL and Siedow JN 1993 Covalent and noncovalent dimers of the cyanide-resistant alternative oxidase protein in higher plant mitochondria and their relationship to enzyme activity. *Plant Physiol.* **103** 845–854

Unger EA and Vasconcelos AC 1989 Purification and characterization of mitochondrial citrate synthase. *Plant Physiol.* **89** 719–723

Varma A and Palsson BO 1994 Stoichiometric flux balance models quantitatively predict growth and metabolic by-product secretion in wild-type *Escherichia coli* w3110. *Appl. Environ. Microbiol.* **60** 3724–3731

van Berlo RJ, de Ridder D, Daran JM, *et al*. 2009 Predicting metabolic fluxes using gene expression differences as constraints. *IEEE/ACM Trans. Comput. Biol. Bioinform.* **8** 206–216

Vanlerberghe GC and McIntosh L 1997 Alternative oxidase: from gene to function. *Annu. Rev. Plant Physiol. Plant Mol. Biol.* **48** 703–734

Vanlerberghe GC 2013 Alternative oxidase: a mitochondrial respiratory pathway to maintain metabolic and signaling homeostasis during abiotic and biotic stress in plants. *Int. J. Mol. Sci.* **14** 6805–6847

Verniquet F, Gaillard J, Neuburger M, *et al*. 1991 Rapid inactivation of plant aconitase by hydrogen peroxide. *Biochem. J.* **276** 643–648

Wang H, Huang J, Liang X, *et al*. 2012 Involvement of hydrogen peroxide, calcium, and ethylene in the induction of the alternative pathway in chilling-stressed *Arabidopsis* callus. *Planta* **235** 53–67

Wedding RT and Black MK 1971 Nucleotide activation of cauliflower α-ketoglutarate dehydrogenase. *J. Biol. Chem.* **246** 1638–1643

Wedding RT, Black MK and Pap D 1976 Malate dehydrogenase and NAD malic enzyme in the oxidation of malate by sweet potato mitochondria. *Plant Physiol.* **58** 740–743

Yuan H, Cheung CM, Poolman MG, *et al*. 2016 A genome-scale metabolic network reconstruction of tomato (*Solanum lycopersicum L.*) and its application to photorespiratory metabolism. *Plant J.* **85** 289–304

Zoglowek C, Kromer S and Heldt HW 1988 Oxaloacetate and malate transport by plant mitochondria. *Plant Physiol.* **87** 109–115

Corresponding editor: Agepati Raghavendra